

## Enhanced ionization of diatomic molecules in strong laser fields: A classical model

D. M. Villeneuve,<sup>\*</sup> M. Yu. Ivanov,<sup>†</sup> and P. B. Corkum

*Steacie Institute for Molecular Sciences, National Research Council of Canada, Ottawa, Ontario, Canada K1A 0R6*

(Received 5 January 1996)

A classical model is developed to study molecular ionization in strong laser fields. The model is compared with a one-dimensional quantum-mechanical model for the case of  $H_2^+$ . The intensity threshold for ionization of  $H_2^+$  is studied as a function of laser polarization, wavelength, pulse duration, and internuclear separation. A range of internuclear separations is found where the ionization rate is enhanced over that at the equilibrium separation, in agreement with the quantum-mechanical model. The classical model is then extended to multi-electron diatomic molecules. A regime is found where simultaneous two-electron ionization occurs. An intensity range is suggested for looking for enhanced ionization effects in dissociating diatomic molecules. [S1050-2947(96)02107-5]

PACS number(s): 33.80.Rv, 42.50.Hz, 33.80.Eh

### I. INTRODUCTION

A number of recent experiments, in which molecules are ionized and dissociated in intense laser fields, have revealed that the kinetic energy of the fragments is consistent with higher ionization states being reached at a critical internuclear separation in the range of 4–5 Å [1–5]. Two explanations have been proposed to explain this puzzling behavior. The first postulates a laser-induced bound molecular state at the critical separation that keeps the nuclei fixed while the electrons are ionized [5]. The second postulates that the molecular ionization rate is enhanced at the critical distance and that ionization to higher charge states occurs as the nuclei pass through this region [6–8].

Quantum-mechanical calculations using the exact three-body Hamiltonian for  $H_2^+$  [9] show that there is indeed a laser-induced avoided crossing that stabilizes the molecule against dissociation; however, the calculation shows that this occurs only at intensities at which ionization will dominate. Furthermore, suppression of dissociation as described in Ref. [9] is only possible because the ground state of  $H_2^+$  is bound; that mechanism does not apply to highly charged ions.

On the other hand, recent quantum-mechanical calculations [10–12] of multiphoton ionization of diatomic molecular ions in an intense laser field have revealed that, in a particular range of internuclear separations  $R$ , the ionization rate is greatly enhanced, in support of the second explanation above. These calculations have recently been corroborated by experiments [13–15].

The quantum calculations are done in a single-active-electron approximation that is rigorously valid only for  $H_2^+$ . For more complex molecular systems or clusters where many electrons are involved in ionization dynamics, the quantum-mechanical calculations of intense-field effects be-

come impractical. Thomas-Fermi-Dirac quantum-mechanical calculations can handle a larger number of electrons, but cannot distinguish between single-electron and multielectron processes, nor can they study sequential versus direct ionization, electron-electron correlations, etc.

Although the interaction of electromagnetic fields with atoms and molecules in principle requires a quantum-mechanical treatment, it has been demonstrated that for the case of intense laser fields a classical treatment may be used. For example, atomic stabilization against ionization in helium has been studied using a classical model [16–18] and harmonic generation in atomic gases has been successfully described with a semiclassical model [19]. Furthermore, simple calculations of over-the-barrier atomic ionization thresholds of noble gases have shown very good agreement with experiments [20].

With intense laser fields, many field-free levels are strongly mixed and participate in the interaction. Energy levels are strongly Stark shifted: for example, at the over-the-barrier ionization threshold for hydrogen ( $1.4 \times 10^{14}$  W/cm<sup>2</sup>), the ponderomotive shift is 16 eV. In the case of diatomic molecules, the motion of the electrons becomes largely perturbed by the external field and the shift of  $\sigma_g$  and  $\sigma_u$  states in  $H_2^+$  is  $\sim 6$  eV at an internuclear separation of 6 bohrs and an intensity of  $1.4 \times 10^{14}$  W/cm<sup>2</sup>. The quantum-mechanical distributions in phase space become very broad and the phases of the wave functions oscillate quickly. Under these conditions, increasingly more classical behavior of the strongly driven quantum system is expected.

Exchange and correlation effects can be missed in the classical approach. While these are important in field-free systems and one-photon ionization processes, they are increasingly difficult to find when the number of photons needed for ionization increases [21]. The search for correlation effects in intense field multiphoton ionization was a major experimental goal since the mid 1980s. A successful observation was made by Fittinghoff [22] in which nonsequential two-electron ionization of helium was observed. However, it was shown both theoretically [19,23] and experimentally [24] that this effect is well described classically.

The above considerations lead us to the purpose of this paper: to determine to what extent a classical model can be

<sup>\*</sup>Electronic address: david.villeneuve@nrc.ca

<sup>†</sup>Also at Department of Chemistry, Carleton University, Ottawa, Ontario, Canada, and Laboratoire de Chimie Théorique, Université Sherbrooke, Sherbrooke, Quebec, Canada J1K 2R1.



FIG. 1. Schematic molecular ion potentials without (left) and with (right) the applied laser field. An electron occupies the left well, while the right well has a net positive charge. The internuclear barrier is lowered by the positive charge of the right well and so at a certain internuclear distance the electron is able to tunnel through the barrier and escape the molecule.

applied to the case of molecules in strong laser fields. We will show that classical calculations yield qualitatively correct results for the behavior of  $\text{H}_2^+$  in intense fields. Using this as a basis, we extend the classical calculation to molecules with several electrons, in order to compare with multiphoton ionization experiments of multielectron diatomic molecules in intense laser fields. Quantum-mechanical calculations for such systems are not possible, even with the best computers available today, which can treat only three degrees of freedom simultaneously in intense fields [9]. We show that enhanced ionization previously described for one-electron molecular systems leads to direct, correlated, multi-electron ionization in a certain region of internuclear separation.

Ionization of a diatomic molecular ion is qualitatively different from that of an atomic ion or a neutral molecule, as illustrated in Fig. 1. If an electron is localized in the upper well and if it has sufficient energy to cross the internal barrier, then it will be able to escape the molecule completely. Because, even in the absence of the laser field, the internuclear barrier is lower than the external one, ionization occurs at a lower intensity than for atoms or neutral molecules.

## II. CLASSICAL CALCULATION

In the classical calculation, we consider a set of  $N$  point particles, with mass  $m_j$  and charge  $q_j$ . For each particle  $j$  we keep track of its position  $\vec{r}_j$  and velocity  $\vec{v}_j$ . The acceleration is calculated from the Coulomb force acting on each particle due to the other  $N-1$  particles and the externally imposed field  $E(t)$ . The particles then move according to Newton's law

$$\frac{d\vec{v}_i}{dt} = \sum_{j \neq i} \frac{q_i q_j}{4\pi m_i \epsilon_0} \frac{(\vec{r}_i - \vec{r}_j)}{(|\vec{r}_i - \vec{r}_j|^2 + \alpha^2)^{3/2}} + \frac{q_i}{m_i} \vec{E}(t), \quad (1a)$$

$$\frac{d\vec{r}_i}{dt} = \vec{v}_i. \quad (1b)$$

Here  $\alpha$  is the smoothing parameter that removes the singularity at  $\vec{r}_i = \vec{r}_j$ . This parameter is routinely used in  $N$ -body problem solvers [25], for example, in galactic cluster calculations, and is necessary in classical simulations of atoms in strong fields [16–18], where the smoothing leads to much better quantitative agreement with fully quantum-mechanical calculations. Smoothing is also necessary to avoid artificial autoionization of multielectron systems, where one of the electrons can be ionized at the expense of the others, which fall below the ground-state energy of the ion. The smoothing parameter is also used in quantum-mechanical calculations [12] discussed below and can be thought of as a consequence of the Heisenberg uncertainty relation.

The set of equations (1) is solved by a fourth-order Runge-Kutta solver with a fixed step size. A fifth-order variable step size algorithm was found to be less efficient because the step size always reduced to that required by the fastest electron. The solver was checked for energy conservation on a field-free helium atom simulation. It was found that the total system energy was maintained within 1% for over 1 ps.

For the results discussed herein, the particles are divided into two classes: mobile electrons and immobile ions. Although the solver is capable of dealing with mobile ions, we are interested in ionization processes as a function of internuclear separation and so the ions are fixed. This simulates experiments with heavy atoms or with very short pulses.

Each simulation generates a set of particle trajectories. An ensemble of trajectories is generated by using a range of initial conditions. The range of initial conditions comes from a single initial position for the electrons at their turning points and allowing the electrons to move in the ionic potentials for a random length of time until the external field is switched on. This yields a microcanonical ensemble that spans all of the initial conditions. An alternative approach to initial conditions is to mimic the ground-state probability distribution by appropriately weighting the initial positions of the electrons. Both of these techniques have been utilized [16–18]; however, because of the difficulty in calculating ground-state wave functions for molecules we chose the former approach.

We similarly chose a simple method to determine when ionization occurred: an electron found to be further than  $10 \text{ \AA}$  from the nearest ion was deemed to be ionized. This technique gives a fairly accurate estimate of the ionization probability in the case of intense laser fields and is simple to implement. In very few cases did an electron beyond this distance recombine with its parent ion. The ionization rates shown below were unaffected when a  $50 \text{ \AA}$  escape radius was used. Quantum-mechanical calculations use a similar method via absorbing boundary conditions and looking at the decrease in the norm of the wave function. In principle it is also possible to look at the total energy of the electrons to determine if they will be able to escape the ion's field. This is more difficult because total energy is not conserved due to the absorption of energy from the strong imposed field. In addition, interactions between the electrons make it difficult

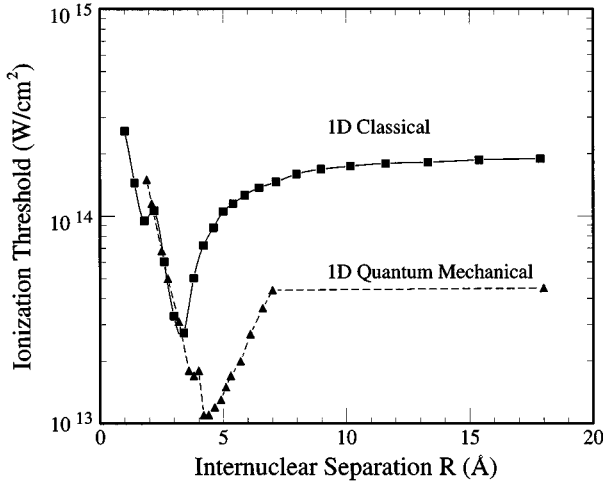


FIG. 2. Intensity threshold for a 50% ionization rate of the  $\text{H}_2^+$  molecular ion, as predicted by the classical model and by a one-dimensional (1D) solution to the Schrödinger equation. Both calculations predict an enhanced ionization at a critical internuclear separation of 3–5 Å. The classical model does not include tunneling and so it predicts a higher ionization threshold at large internuclear separation, corresponding to the hydrogen atom. This also accounts for the discrepancy in the location of the minima.

to predict if an electron that has sufficient kinetic energy will actually escape the ion's field.

### III. $\text{H}_2^+$ SIMULATIONS

For the  $\text{H}_2^+$  simulation, there are two fixed ions of unit charge separated by a distance  $R$  and a single mobile electron initially bound to one ion with the correct ionization potential. The laser pulse shape was chosen to be

$$\vec{E}(t) = \vec{E}_0 \sin(\pi t/t_p) \sin \omega_L t \quad (0 \leq t \leq t_p), \quad (2)$$

where  $\vec{E}_0$  is the peak field,  $t_p$  is the full width of the pulse duration, and  $\omega_L$  is the laser frequency, chosen to correspond to a wavelength of 750 nm. The sinusoidal pulse envelope has the advantage of having a distinct starting and stopping time, unlike a Gaussian envelope.

For each value of laser intensity and internuclear separation, a set of trajectories is computed. The ionization probability is derived from the fraction of electrons that escapes the ions. In Fig. 2 we show the intensity at which ionization occurs 50% of the time, as a function of internuclear separation. Also shown in the figure is the threshold calculated by numerically solving the time-dependent Schrödinger equation in one dimension; the ionization rate is measured from the time decay of the norm [12]. Both of these calculations were one dimensional.

At infinite  $R$ , ionization of  $\text{H}_2^+$  reduces to ionization of H. The classical calculation for the ionization threshold for the hydrogen atom is very close to the over-the-barrier value obtained analytically in the static field limit [20],  $I = 1.4 \times 10^{14} \text{ W/cm}^2$ . The tunneling “threshold” for H by integrating the Keldysh formula over the pulse envelope is  $1.2 \times 10^{14} \text{ W/cm}^2$ . The classical threshold is consistently higher than the quantum-mechanical one, because the latter

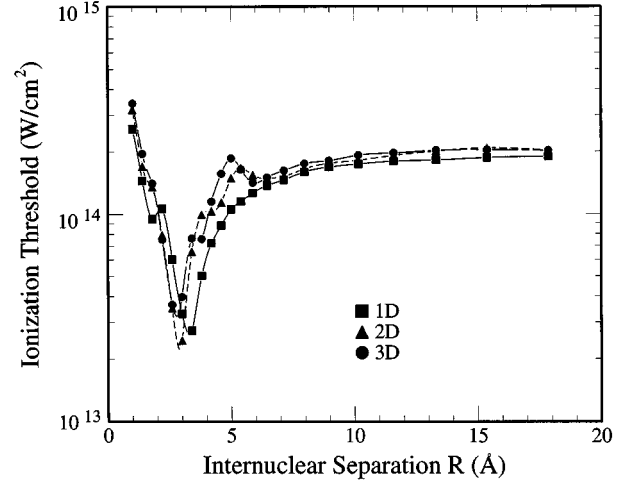


FIG. 3. Effects of dimensionality of the classical model on the ionization threshold for  $\text{H}_2^+$ . The only significant change is near 5 Å, where the one-dimensional model predicts a higher ionization rate.

includes tunneling through the barrier and multiphoton ionization. The quantum-mechanical ionization rate will be substantially lower when calculated in three dimensions [26], which will reduce the discrepancy between the classical and quantum predictions.

The usual numerical tests were performed to verify the accuracy of the solution. For instance, the time step was reduced to check the convergence. The sensitivity to the smoothing parameter  $\alpha$  was tested by changing its value while changing the initial electron position to maintain the ionization potential. In all instances of changed parameters, the shape of the curve remained as in Fig. 2, except for minor shifts in the fine structure.

The dimensionality of the classical calculation also had little effect on the threshold. Figure 3 shows the ionization threshold for one, two, and three dimensions. The effect of laser field polarization on the threshold is much more evident. Figure 4 shows the ionization threshold for linearly polarized light aligned along the internuclear axis, aligned perpendicular to the internuclear axis, and for circularly polarized light. Clearly, the enhanced ionization requires a laser field component parallel to the internuclear axis.

There is very little difference in ionization threshold when the pulse duration (full width) is changed from 30 to 100 fs. This is because the ionization is a highly nonlinear function of intensity, but a linear function of time. The shape of the threshold curve also remained similar for wavelengths of 300 and 1064 nm.

The results of a classical model can be viewed and interpreted directly. One can observe the trajectory of the electron in the laser field to understand the ionization process. In the case of  $\text{H}_2^+$ , three regimes are identified: (a) For small internuclear separations the electron is able to move freely between nuclei, (b) at large internuclear separations the electron is localized on one nucleus and it behaves as H, and (c) at the intermediate internuclear separation where enhanced ionization occurs, the electron is seen to hop between nuclei, and as it ionizes it starts at the high potential side, hops the internuclear barrier, and quickly passes the other nucleus before escaping.

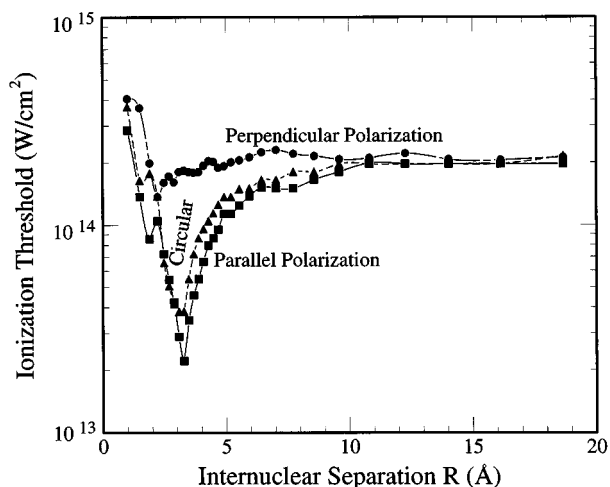


FIG. 4. Effects of laser polarization direction as compared with the internuclear axis of  $H_2^+$ . Enhanced ionization is only evident when the laser field has a component parallel with the internuclear axis.

We can also study diatomic molecules in higher charge states. For example, in Fig. 5 we see the enhanced ionization of  $He_2^{3+}$ , which exhibits similar behavior to that of  $H_2^+$ .

#### IV. $H_2$ SIMULATION

At this point, we have established that the classical model makes qualitatively similar predictions to the quantum-mechanical model in the case of  $H_2^+$ . We now extend the model to systems with more than one electron, systems that are more difficult to treat quantum mechanically. In particular, we are interested in how strong field ionization occurs in neutral diatomic molecules, when the enhancement mechanism seen in  $H_2^+$  is not yet available to the molecule.

In Fig. 6 we show the intensity threshold for ionizing the first and second electrons from  $H_2$ . The lower curve is the intensity at which there is a 50% probability that one electron is detached and the upper curve is for a 50% probability

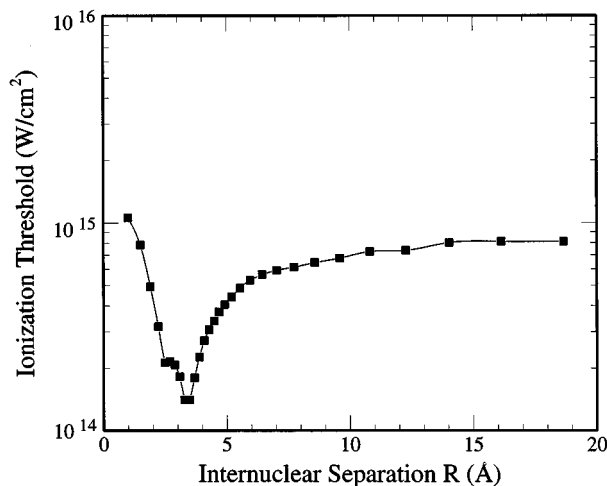


FIG. 5. Increasing the nuclear charge from 1 (for  $H_2^+$ ) to 3 (for  $He_2^{3+}$ ) has little effect on the critical internuclear distance, but it increases the ionization threshold because of the stronger binding.

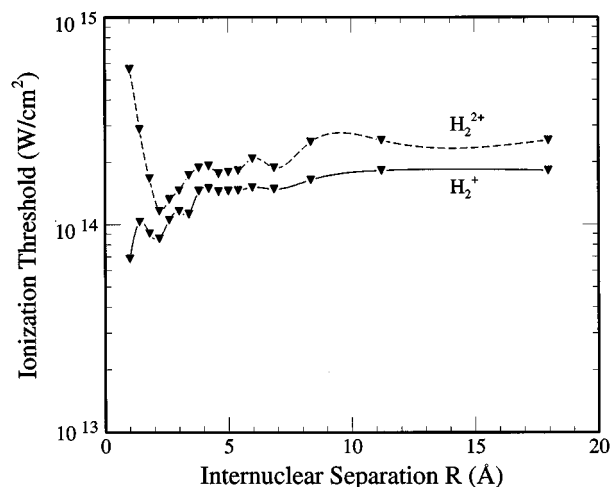


FIG. 6. Ionization threshold for the neutral  $H_2$  molecule. The lower curve represents the intensity at which there is a 50% probability that one electron is detached. The upper curve is the 50% probability threshold that two electrons are detached. In the case of a neutral molecule, there is no enhancement mechanism and so the threshold for the first ionization is about the same as for the hydrogen atom. When the first electron escapes, the resulting  $H_2^+$  molecular ion is then above threshold for losing its remaining electron.

that two electrons are detached. The pronounced enhancement seen in  $H_2^+$  is not evident here because the enhancement mechanism does not become available until the first electron escapes. An intensity of  $2 \times 10^{14}$  W/cm<sup>2</sup> is required to remove the first electron, much like the lone hydrogen atom, at which point the molecule finds itself as  $H_2^+$ . Comparing with Fig. 2, we see that this intensity is above the ionization threshold for  $H_2^+$  for all but the smallest internuclear separation and thus we expect that the second electron will be ionized at the same intensity, as is seen.

To look for evidence of simultaneous ionization, a number of simulations were run for an intensity of  $6 \times 10^{14}$  W/cm<sup>2</sup> with a 30 fs full-width pulse, at three internuclear separations, and the time at which each electron escaped was recorded. When the time delay between the first and the second ionization is plotted as a histogram (Fig. 7), it is seen that at  $R = 3.5$  Å the two electrons are clearly correlated, with the second one usually escaping within one-quarter of an optical cycle of the first one. This is evidence of correlated electron emission from molecules.

It should also be noted that this effect is wavelength dependent. If a longer laser wavelength were used, the probability of correlated two-electron detachment would be higher, and this is something that might be observable in CO<sub>2</sub> laser experiments.

#### V. $He_2$ SIMULATION

Many high-intensity experiments use larger diatomic molecules than  $H_2$ ; for example,  $I_2$  is often studied. How will enhanced ionization manifest itself? We now model a diatomic system with four valence electrons, nominally  $He_2$ . Again, the nuclei are frozen, which, for a molecule like  $I_2$ , is a good approximation.

In Fig. 8 the intensities at which each of the charge states

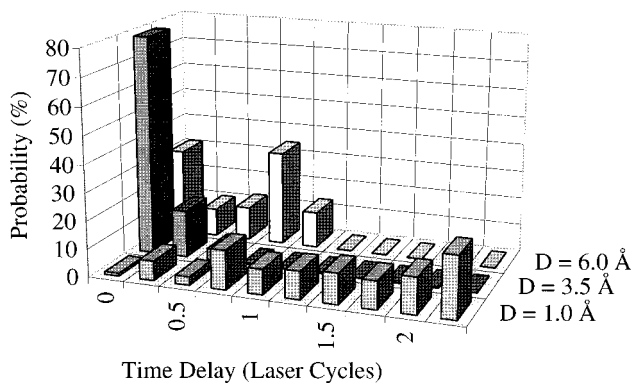


FIG. 7. Histograms of correlations between the ionization times of the first and second electrons in  $H_2$ , for three internuclear distances, and at an intensity of  $6 \times 10^{14}$   $W/cm^2$ . The height of each bar represents the probability that the second electron will escape within that quarter-cycle of the laser field following the first electron's escape. At  $D = 3.5$  Å, the second electron escapes within one-quarter cycle of the first electron, and we can say that this is correlated two-electron emission.

appears are shown. The enhancement in ionization rate is only significant for the higher charge states. If one were to devise an experiment to study enhanced ionization by dissociating  $I_2$  and ionizing it as it dissociates, an intensity in the mid  $10^{14}$   $W/cm^2$  range is needed, and one should look for ions such as  $I^{2+}$  and higher.

## VI. MOBILE IONS

Up to this point, we have assumed that the nuclei are frozen, that is, they do not move on the time scale of the laser pulse. However, real experiments must deal with mov-

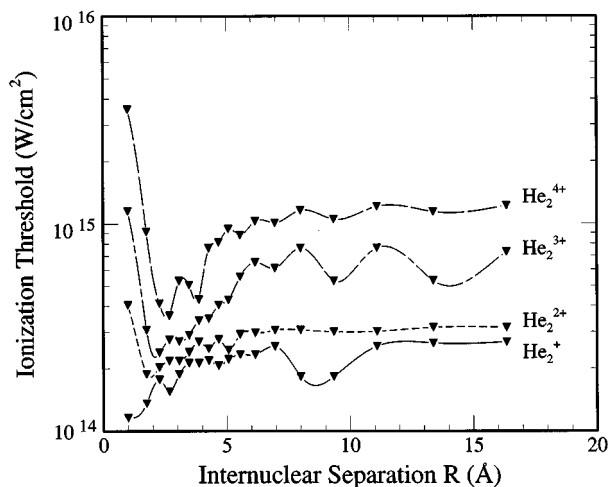


FIG. 8. Ionization threshold to reach various ionization states of  $He_2$ . (This represents any diatom with a total of four valence electrons.) Like the case of  $H_2$ , there is little apparent enhancement of the first ionization, but by the third ionization the rate is clearly enhanced near the critical internuclear distance. This suggests that, in doing ionization experiments with neutral molecules such as  $I_2$ , one should look for evidence of enhanced ionization in the more highly charged products.

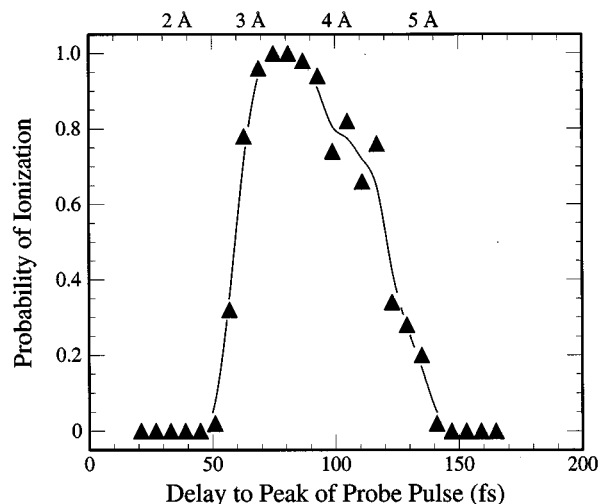


FIG. 9. Probability of ionization of dissociating  $H_2^+$ , as a function of time delay between the start of dissociation and the peak of the ionizing laser pulse. The intensity was  $7 \times 10^{13}$   $W/cm^2$ . This is different from the simulations shown earlier in that the ions are now able to move self-consistently in the field. The approximate internuclear distance at each time is shown at the top. This simulates recent experiments where dissociating  $I_2^+$  shows an enhanced ionization rate near the critical separation.

ing ions and so we now consider the  $H_2^+$  system with mobile ions. We are interested in comparing the code predictions with the results of Constant *et al.* [13], in which  $I_2^+$  was produced by one laser pulse and was further ionized by a second laser pulse. An enhanced ionization rate was observed when the time delay between the two pulses corresponded to the nuclei being at the critical internuclear distance of 4–5 Å.

We use Eq. (1), but now permit the ions to move. Some care must be taken in choosing the initial conditions.  $H_2^+$  can form a bound state in the field-free case and the nuclei vibrate about an equilibrium position. The initial internuclear separation was chosen so that the molecule had sufficient potential energy to dissociate.

At time zero the nuclei begin to move apart and at a given time delay the laser pulse turns on and the probability of ionization is measured. Figure 9 shows the ionization probability as a function of delay time and also includes the approximate internuclear distance at each time. Although details such as dissociation velocity cannot be directly compared with the experiment, it can be seen that the ionization rate peaks strongly at the critical internuclear distance. This supports the experimental observations of Constant *et al.* and validates the calculations made above with immobile ions.

## VII. CONCLUSIONS

A simple classical model of molecular ionization is shown to give similar results to a one-dimensional quantum-mechanical model. The classical model is then extended to multielectron diatomic molecules. A range of internuclear separations is found in which the ionization rate is greatly enhanced. A regime where two electrons are simultaneously

detached is observed. An intensity range for future experiments on  $I_2$  is proposed. The model is tested with nuclear motion included for a simple dissociating molecule and the predictions agree qualitatively with recent experimental observations.

This model can be extended to larger molecules and to study Coulomb explosions of molecules. It can also be used to investigate electron heating effects in clusters that have

been shown to have anomalously high electron temperatures [27–29].

#### ACKNOWLEDGMENTS

The authors acknowledge stimulating discussions with K. Rzażewski and T. Seideman. M.I. acknowledges financial support from an NSERC collaborative grant.

- 
- [1] C. Cornaggia, J. Lavancier, D. Normand, J. Morellec, P. Agostini, J. P. Chambaret, and A. Antonetti, *Phys. Rev. A* **44**, 4499 (1991).
- [2] C. Cornaggia, D. Normand, and J. Morellec, *J. Phys. B* **25**, L415 (1992).
- [3] L. J. Frasinski, P. A. Hatherly, K. Codling, M. Larsson, A. Persson, and C.-G. Wahlstrom, *J. Phys. B* **27**, L109 (1994).
- [4] P. A. Hatherly, M. Stankiewicz, K. Codling, L. J. Frasinski, and G. M. Cross, *J. Phys. B* **27**, 2993 (1994).
- [5] M. Schmidt, D. Normand, and C. Cornaggia, *Phys. Rev. A* **50**, 5037 (1994).
- [6] K. Codling, L. J. Frasinski, and P. A. Hatherly, *J. Phys. B* **22**, L321 (1995).
- [7] J. H. Posthumus, L. J. Frasinski, A. J. Giles, and K. Codling, *J. Phys. B* **28**, L349 (1995).
- [8] S. Chelkowski and A. D. Bandrauk, *J. Phys. B* **28**, L723 (1995).
- [9] S. Chelkowski, T. Zuo, O. Atabek, and A. D. Bandrauk, *Phys. Rev. A* **52**, 2977 (1995).
- [10] T. Zuo, S. Chelkowski, and A. D. Bandrauk, *Phys. Rev. A* **48**, 3837 (1993).
- [11] T. Zuo and A. D. Bandrauk, *Phys. Rev. A* **52**, 2511 (1995).
- [12] T. Seideman, M. Yu. Ivanov, and P. B. Corkum, *Phys. Rev. Lett.* **75**, 2819 (1995).
- [13] E. Constant, H. Stapelfeldt, and P. B. Corkum, *Phys. Rev. Lett.* (to be published).
- [14] D. Normand and M. Schmidt, *Phys. Rev. A* **53**, 1958 (1996).
- [15] F. A. Ilkov, T. D. G. Walsh, S. Turgeon, and S. L. Chin, *Phys. Rev. A* **51**, R2695 (1995).
- [16] J. Grochmalicki, M. Lewenstein, and K. Rzażewski, *Phys. Rev. Lett.* **66**, 1038 (1991).
- [17] M. Gajda, J. Grochmalicki, M. Lewenstein, and K. Rzażewski, *Phys. Rev. A* **46**, 1638 (1992).
- [18] K. Rzażewski, M. Lewenstein, and P. Salières, *Phys. Rev. A* **49**, 1196 (1994).
- [19] P. B. Corkum, *Phys. Rev. Lett.* **71**, 1994 (1993).
- [20] S. Augst, D. Strickland, D. D. Meyerhofer, S. L. Chin, and J. H. Eberly, *Phys. Rev. Lett.* **63**, 2212 (1989).
- [21] N. B. Delone and V. P. Krainov, *Multiphoton Processes in Atoms* (Springer-Verlag, Berlin, 1994).
- [22] D. Fittinghoff, P. Bolton, B. Chang, and K. Kulander, *Phys. Rev. Lett.* **69**, 2642 (1993).
- [23] T. Brabec, M. Ivanov, and P. B. Corkum (unpublished).
- [24] P. Dietrich, N. H. Burnett, M. Ivanov, and P. B. Corkum, *Phys. Rev. A* **50**, 50 (1994).
- [25] *Multiple Time Scales*, edited by Jeremiah U. Brackbill and Bruce I. Cohen (Academic, Orlando, 1985).
- [26] A. Bandrauk (private communication).
- [27] C. Wulker, W. Theobald, D. Ouw, F. P. Schafer, and B. N. Chichkov, *Opt. Commun.* **112**, 21 (1994).
- [28] A. McPherson, B. D. Thompson, A. B. Borisov, K. Boyer, and C. K. Rhodes, *Phys. Rev. Lett.* **72**, 1810 (1994).
- [29] J. Purnell, E. M. Snyder, S. Wei, and A. W. Castleman, *Chem. Phys. Lett.* **229**, 333 (1994).